Immunity, Volume *33*

Supplemental Information

Plasmacytoid Dendritic Cell Ablation Impacts Early Interferon Responses and Antiviral NK and CD8$^+$ T Cell Accrual

Melissa Swiecki, Susan Gilfillan, William Vermi, Yaming Wang, and Marco Colonna

Inventory of Supplemental Information

Figure S1, related to Figure 1. Generation of SiglecH-eGFP gene-targeted mice and depletion of pDCs. This figure shows the construct for SiglecH-eGFP gene-targeted mice and demonstrates that (i) GFP is not restricted to pDCs and (ii) when crossed to BDCA2-DTR Tg mice, pDCs (GFP^{hi}) but not classical DCs (GFP^{lo}) are selectively depleted.

Figure S2, related to Figure 2. pDC activation and DT-mediated depletion during MCMV infection. This figure illustrates that pDCs are systemically activated and can be effectively depleted during MCMV infection. It also shows that other cell types critical for antiviral responses are not depleted in BDCA2-DTR Tg mice by DT administration.

Figure S3, related to Figure 3. Activation of NKT cells during MCMV infection. This figure shows that depletion of pDCs impacts NKT responses during MCMV infection.

Figure S4, related to Figure 5. pDCs are systemically activated during VSV-OVA infection. This figure shows that pDCs are systemically activated in vivo by VSV-OVA.

Figure S5, related to Figure 7. Impact of pDC depletion on classical DCs in VSV-infected mice. This figure shows that pDC depletion during VSV-OVA infection does not affect classical DC numbers or their ability to present antigen to T cells from TCR Tg mice ex vivo.

Supplemental Methods. Detailed methods describing virus plaque assays and reagents used for flow cytometric analyses.

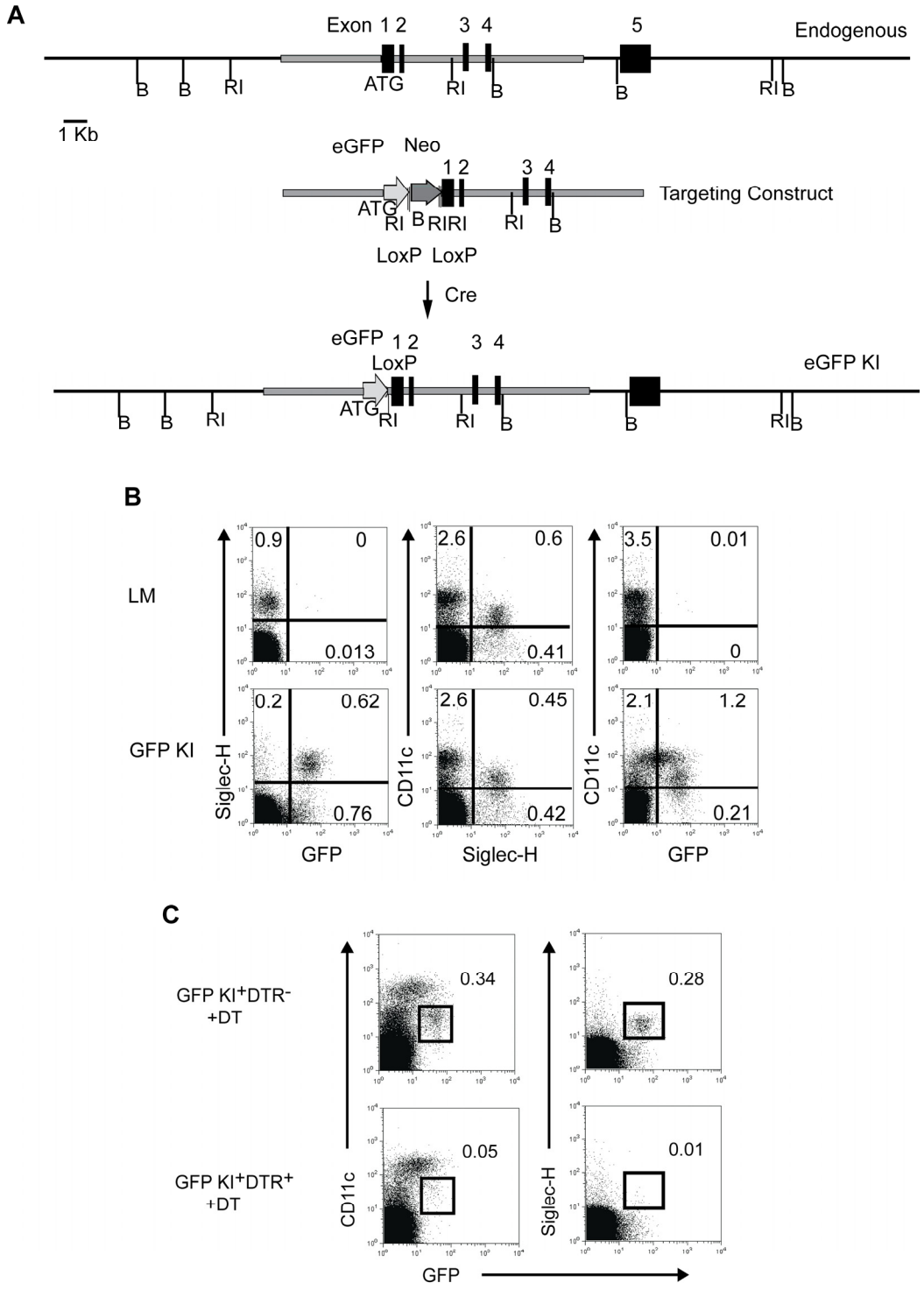

Figure S1, related to Figure 1. Generation of SiglecH-eGFP gene-targeted mice and depletion of pDCs. (A) Construct for SiglecH-eGFP gene-targeted mice. A cDNA fragment encoding eGFP was inserted right after the ATG of the Siglec-H gene (B, BamHI; RI, EcoRI; Neo, neomycin). (B) GFP expression in pDCs and CD11c^{hi} DCs. Spleen cells from SiglecH-eGFP heterozygous mice (GFP KI) and littermate controls (LM) were analyzed for Siglec-H, B220 and GFP expression by flow cytometry. (C) SiglecH-eGFP mice were crossed to BDCA2-DTR Tg mice and treated with DT. DT eliminates pDCs (Siglec-H^{+}CD11c^{lo}GFP^{hi}) but not classical DCs (Siglec-H^{-} CD11c^{hi}GFP^{lo}) in spleens 24 hr postinjection. Data shown are representative of at least three experiments.

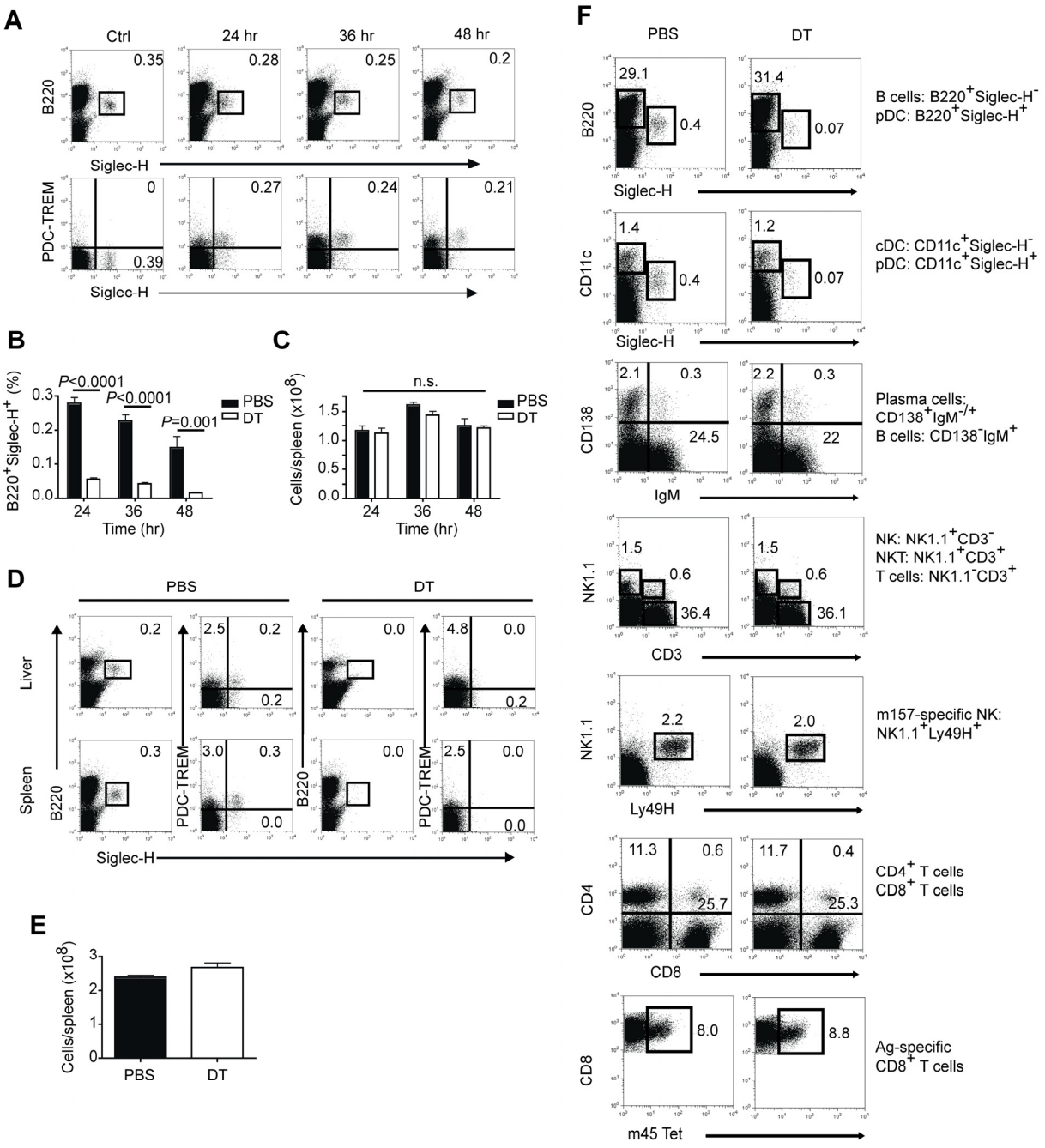

Figure S2, related to Figure 2. pDC activation and DT-mediated depletion during MCMV infection. MCMV activates pDCs in vivo. (A) pDCs ($B220^+Siglec\text{-}H^+$) from spleens of MCMV-infected ($5x10^4$ pfu, i.p.) mice were analyzed for the expression of PDC-TREM by flow cytometry. Dot plots are representative of five to six mice per group. (B,C) pDCs are effectively depleted during MCMV infection. (B) Frequencies of $B220^+Siglec\text{-}H^+$ pDCs and (C) total cell numbers in spleens of PBS or DT-treated mice. *P* value, unpaired, two-tailed Student's *t*-test; not significant (n.s.). Data are from two experiments (mean ± SEM, n=5-6). (D) Liver and spleen cells from control or pDC-depleted MCMV-infected mice were analyzed for Siglec-H, B220 and PDC-TREM expression by flow cytometry 36 hr p.i. Dot plots are representative of five to six mice per group. (E,F) Mice were injected i.p. with MCMV ($5x10^4$ pfu) then administered PBS or DT on day 6 p.i. (E) Cells/spleen on day 7 p.i. (mean +/- SEM, n=3). (F) Spleen cells were stained on day 7 p.i. with a panel of antibodies to distinguish specific lymphocyte populations including MCMV-specific NK cells and $CD8^+$ T cells. Dot plots are representative of three mice per group.

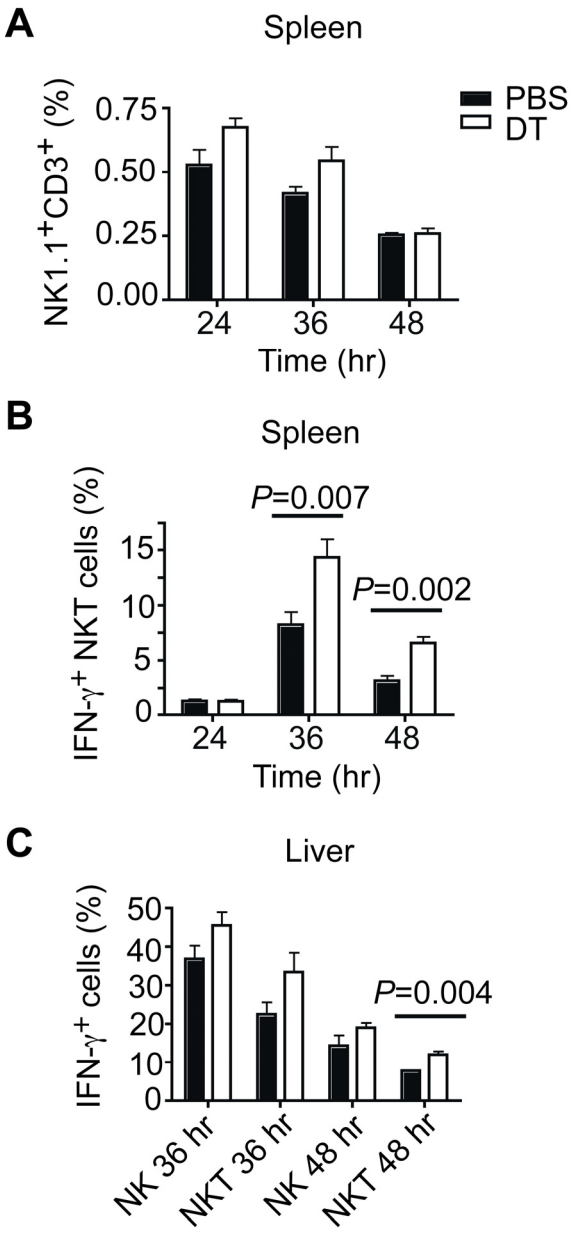

Figure S3, related to Figure 3. Activation of NKT cells during MCMV infection. (A) Frequencies of NK1.1^{+}CD3^{+} NKT cells in spleens of PBS or DT-treated mice infected i.p. with MCMV (5x10^{4} pfu). (B) Frequencies of spleen NKT cells producing IFN-γ. (C) Frequencies of liver NK (NK1.1^{+}CD3^{-}) and NKT cells producing IFN-γ. *P* value, unpaired, two-tailed Student's *t*-test. Data are from two experiments (mean ± SEM, n=5-7).

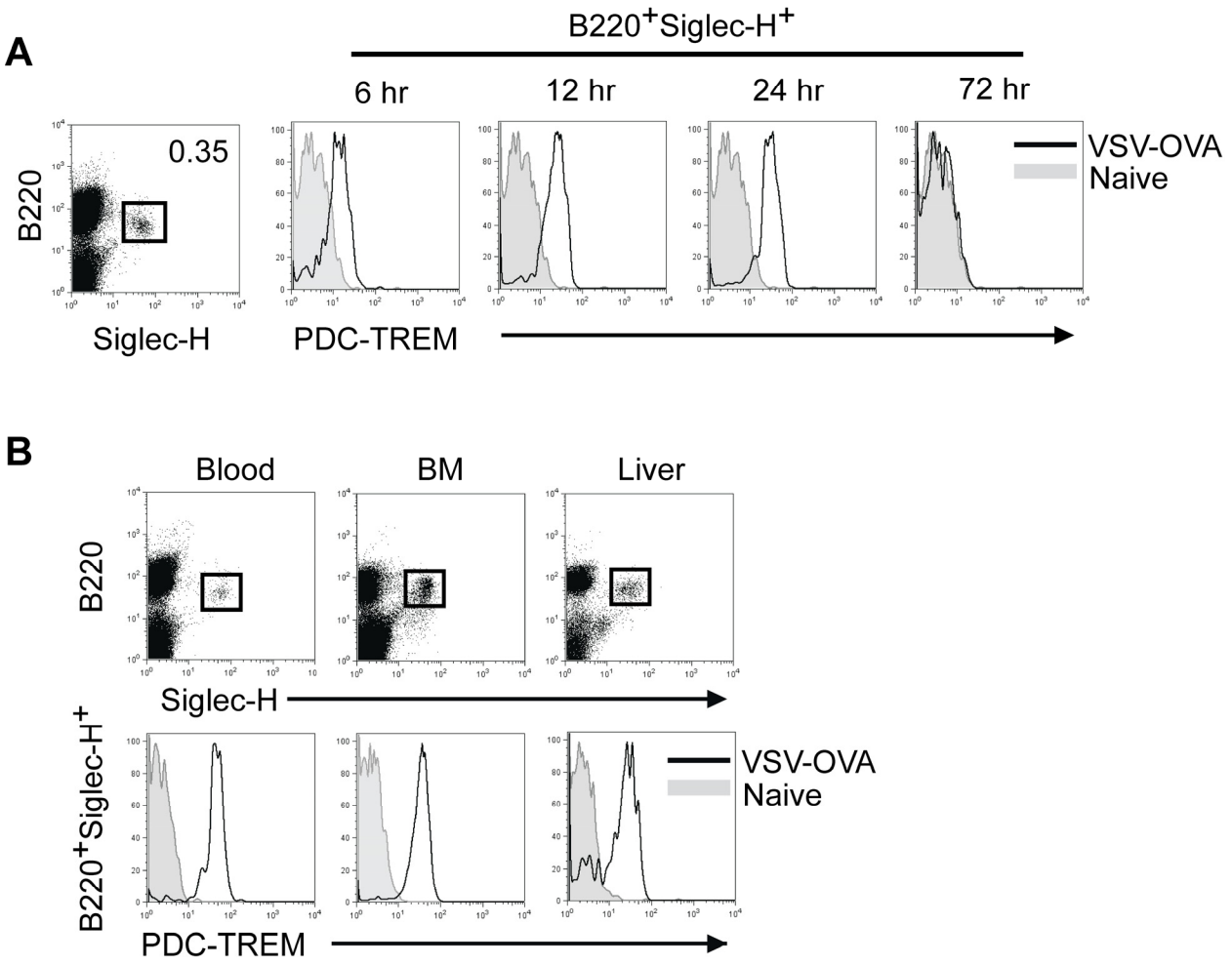

Figure S4, related to Figure 5. pDCs are systemically activated during VSV-OVA infection. Mice were infected i.v. with VSV-OVA and PDC-TREM expression on $B220^{+}Siglec\text{-}H^{+}$ pDCs was analyzed by flow cytometry. (A) PDC-TREM expression on spleen pDCs at different timepoints p.i. (B) PDC-TREM expression on pDCs from blood, bone marrow (BM) and liver 24 hr p.i. Data are representative of three experiments.

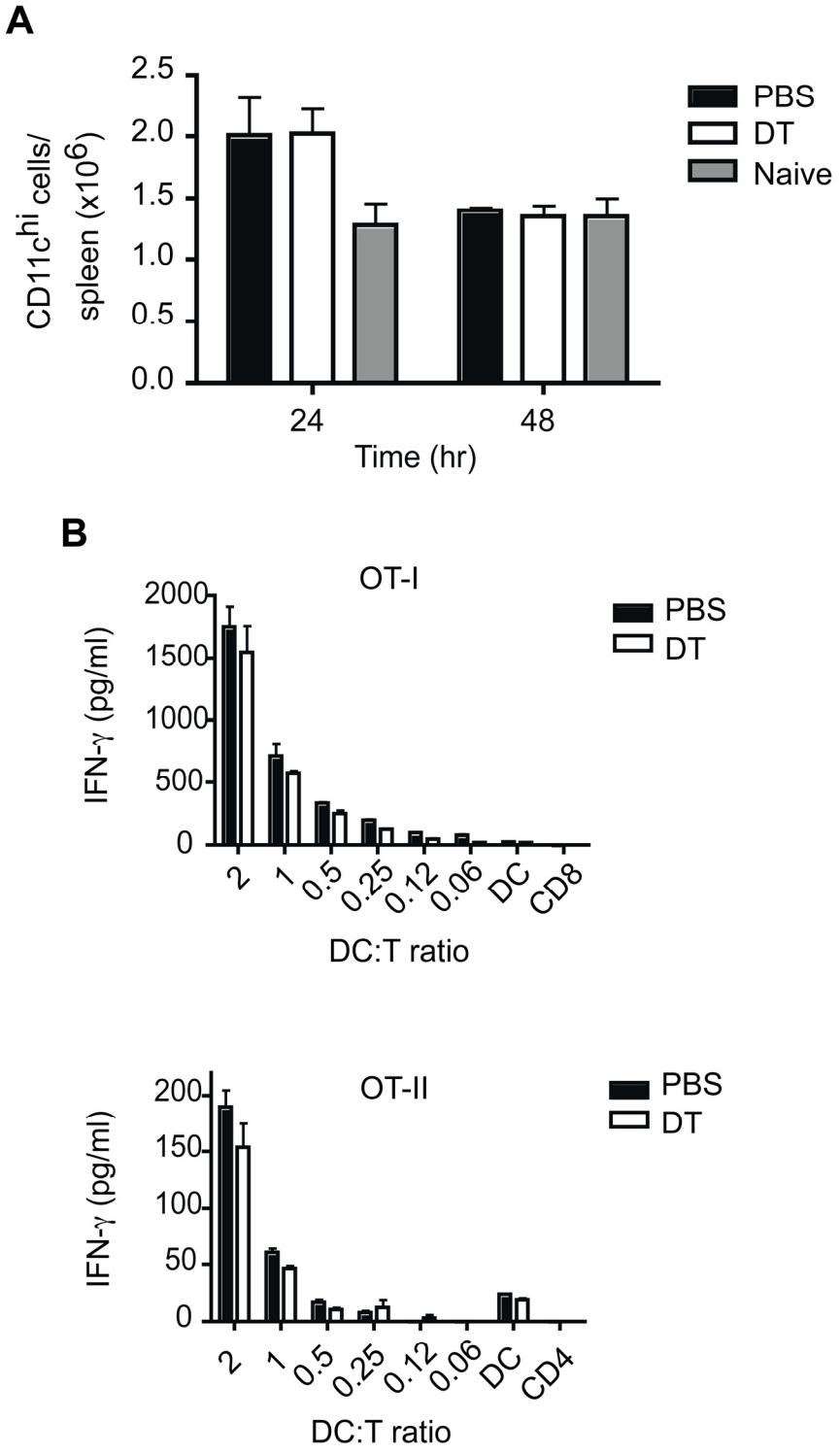

Figure S5, related to Figure 7. Impact of pDC depletion on classical DCs in VSV-infected mice. Mice were infected i.v. with VSV-OVA. (A) DC ($CD11c^{hi}$) numbers in spleens of PBS or DT-treated mice at 24 and 48 hr p.i. (mean ± SEM, n=4). (B) Ag presentation to OT-I and OT-II cells. $CD11c^{hi}$ cells were enriched from spleens of PBS or DT-treated mice 24 hr p.i. and co-cultured for 48 hr with $CD8^+$ or $CD4^+$ T cells purified from OT-I or OT-II TCR Tg mice, respectively. IFN-γ in supernatants was measured by CBA. Data are representative of two experiments where DCs were enriched or sorted from five mice per group.

Supplemental Experimental Procedures

Virus plaque assays. MCMV titers were determined by standard plaque assay. Briefly, organs from MCMV-infected mice were collected and stored at -80ºC in 1 ml complete DMEM with zirconia-silica beads (BioSpec). Organs were thawed quickly at 37ºC then homogenized with a Roche MagNA Lyser. Monolayers of 3T12 cells in 12-well plates were infected with serial dilutions of homogenates in duplicate. After incubation for 1 hr at 37ºC cells were covered with an overlay of 2x complete DMEM plus 3% SeaPlaque agarose (1:1) (Lonza). Cells were overlaid again on day 3 with 2x complete DMEM plus 3% SeaKem agarose (1:1) (Lonza) and neutral red. On day 4 plaques were counted using a light microscope. For VSV-OVA titers, spleens were collected and stored at -80ºC in plain DMEM. Samples were thawed, homogenized and diluted as described above. Vero cell monolayers were infected in 12-well plates for 1 hr. After incubation, cells were overlaid with 2x complete DMEM plus 2% methyl cellulose (1:1). After 18-20 hr, cells were overlaid again with phosphate buffered saline plus neutral red. Plaques were counted using a light microscope 8-12 hr later.

Antibodies and flow cytometry. The following reagents were from BD Biosciences, Biolegend or Miltenyi Biotec: fluorochrome labeled anti-Siglec-H (551), anti-B220 (RA3-6B2), anti-CD11c (HL3), anti-CD8α (53-6.7), anti-CD4 (GK1.5), anti-CD40 (3/23), anti-CD80 (16-10A1), anti-CD86 (GL1), anti-I-A^b (AF6-120.1), anti-CD3 (145-2C11), anti-NK1.1 (PK136), anti-Ly49H (3D10), anti-IFN-γ (XMG1.2), anti-IL-12 (C15.6), anti-Vα2 (B20.1), anti-CD11b (M1/70), anti-CD115 (AFS98), anti-Ly6C (AL-21), anti-mPDCA-1 (JF05-1C2.4.1), anti-IgM (II/41), anti-CD138 (281-2) and Streptavidin. Anti-PDC-TREM (clone 162.7, rat IgG2a), anti-Siglec-H (clone 440c, rat IgG2b) and anti-BST-2 (clone 927, rat IgG2b) antibodies were purified from ascites and biotinylated using the Fluororeporter Minibiotin Kit (Invitrogen). Ag-specific $CD8^+$ T cells in mice infected with VSV-OVA were detected with H-$2K^b$ $OVA_{257-264}$ peptide tetramers (Beckman Coulter). The H-$2D^b$ m45

tetramer used to detect Ag-specific $CD8^+$ T cells in MCMV-infected mice was a generous gift from Mike Brown (University of Virginia, Charlottesville, VA). Intracellular staining for IFN-γ and IL-12 were performed using the BD Cytofix-Cytoperm kit (BD Biosciences) according to the manufacturer instructions. Splenocytes from MCMV-infected mice were incubated for 6 hr with brefeldin A prior to IL-12 or IFN-γ intracellular staining. Intracellular IFN-γ content of NK cells and NKT cells during MCMV infection was examined using freshly isolated cells except on day 3 p.i. Fc receptors were blocked before surface staining with supernatant from HB-197 cells (ATCC) and dead cells were excluded with propidium iodide. All flow cytometry was conducted on a dual laser FACSCalibur flow cytometer (BD Biosciences) and analyzed with FlowJo software (Tree Star, Inc.).